J Mater Sci (2010) 45:6170–6173
DOI 10.1007/s10853-010-4707-x

Effect of sample geometry on the deformation behavior of Zr-based bulk metallic glass

N. H. Tariq · J. I. Akhter · B. A. Hasan

Received: 1 February 2010 / Accepted: 8 June 2010 / Published online: 22 June 2010

Abstract In this study, effect of geometrical confinement on the deformation behavior of $Zr_{57.5}Cu_{11.2}Ni_{13.8}Al_{17.5}$ bulk metallic glass (BMG) was investigated. For this purpose flat top conical samples with different semi-vertex angles (α) were prepared for quasi-static compression tests. It was observed that as the geometry of the sample is slightly changed from cylindrical shape (for which $\alpha = 0°$) to conical shape (for which $\alpha > 0°$), a brittle BMG sample tends to deform in a ductile manner due to the geometrical constraint-induced complex multi-axial stress distribution in the sample. In brittle $Zr_{57.5}Cu_{11.2}Ni_{13.8}Al_{17.5}$ specimen with $\alpha = 5°$, plastic deformation of about 4% was observed due to the formation of extensive intersecting shear bands.

Introduction

Bulk metallic glasses (BMGs), which possess many attractive properties including high strength, elastic deformability, and corrosion resistance, have great application potentials as structural and functional materials [1–3]. However, the room temperature brittleness of BMGs is still one of the most serious problems which limit their real engineering applications [4–11]. The brittleness of BMGs is attributed to the highly localized inhomogeneous deformation behavior. Nucleation of primary shear bands occurs preferentially in the direction of maximum shear stress upon yielding and further plastic deformations are highly localized in these bands. In an unconstrained geometry, failure of BMGs occurs catastrophically on one dominant shear band [10, 12, 13]. In order to understand the mechanism of plastic deformation in BMGs, various strategies have been adopted to avoid the rapid propagation of shear bands and to generate multiple shear bands by geometrically confining the sample [7, 10, 11, 13–20]. In this study, flat top conical specimens of $Zr_{57.5}Cu_{11.2}Ni_{13.8}Al_{17.5}$ BMG having specific dimensions were prepared for compression test and the brittle BMG sample deformed plastically. Under this configuration, multiple shear bands were generated in the monolithic BMG sample with a considerable displacement prior to failure. It is expected that the findings of this study would be very useful for engineering applications and processing of BMGs.

N. H. Tariq (✉) · B. A. Hasan
Powder Metallurgy Lab, Department of Chemical and Materials Engineering, Pakistan Institute of Engineering and Applied Sciences, P.O. Nilore, Islamabad, Pakistan
e-mail: naeem421@hotmail.com

J. I. Akhter
Physics Division, Pakistan Institute of Nuclear Science and Technology, P.O. Nilore, Islamabad, Pakistan

Experimental

Button of $Zr_{57.5}Cu_{11.2}Ni_{13.8}Al_{17.5}$ alloy was prepared by arc melting of high-purity Zr (4 N), Cu (4 N), Ni (4 N), and Al (4 N) under Ti-getter-purified argon atmosphere. The sample was remelted four times to improve homogeneity. This button was finally remelted and suction-cast into rod-shape sample of dimensions 3 mm × 50 mm in copper die.

The rod was machined to produce flat top conical samples having dimensions and conical geometry as shown in Fig. 1. Low-temperature differential scanning calorimetry (DSC) was performed using TA INSTRUMENTS/DSC-Q100 at a heating rate of 20 K/min to evaluate thermal parameters for the alloy. X-ray diffraction (XRD) of the alloy was conducted by Shimadzu XRD-6000 using

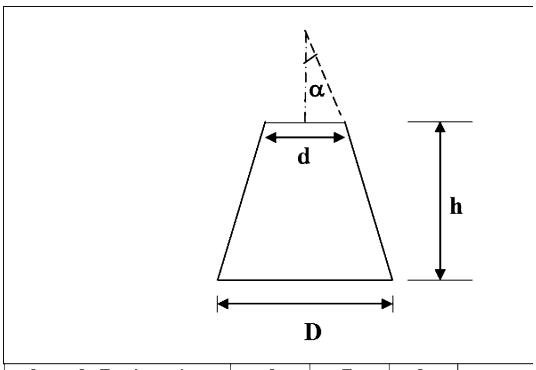

Sample Designation	d (mm)	D (mm)	h (mm)	α (deg.)
Sample 1 (Cylinderical)	3	3	6	0
Sample 2 (Conical)	2.5	3	6	2
Sample 3 (Conical)	2	3	6	5

Fig. 1 Geometry and dimensions of conical BMG samples

Cu Kα_1 radiation ($\lambda = 1.54060$ Å) to confirm the amorphous nature of the alloy. Compression test was conduced under uniaxial compressive quasi-static loading at a constant strain rate of 4.2×10^{-4} s^{-1} using specially designed conical samples having aspect ratio of 2. Finally, fractured surfaces of compression tested samples were examined in scanning electron microscope (SEM).

Results and discussions

XRD pattern of as-cast sample is shown in Fig. 2. A halo region indicative of amorphous structure was observed. Low-temperature DSC plot of the alloy at a heating rate of 20 K/min is shown as an inset of Fig. 2. DSC trace shows a single endothermic peak, indicating the glass transition T_g, and an exothermic peak showing single stage crystallization reaction in the alloy. This also confirms amorphous nature of the alloy. The glass transition temperature, T_g, and onset temperature of exothermic reaction, T_x, were found to be 703 and 776 K, respectively.

Figure 3 shows load–displacement curves for as-cast cylindrical specimen (sample 1) and conical samples with semi-vertex angle (α) of 2° (sample 2) and 5° (sample 3). It is quite clear from Fig. 3 that the as-cast $Zr_{57.5}Cu_{11.2}Ni_{13.8}Al_{17.5}$ BMG sample having conventional cylindrical geometry is fractured in a brittle manner at a load of 12.6 kN. On the other hand conical samples showed distinct mechanical response. They not only showed considerable plastic deformation, but also had increased fracture strength. The conical samples with $\alpha = 2°$ yielded at a load of 12 kN. After yielding, the alloy showed displacement of about 0.1 mm and then fractured at a load of 13 kN. In case of sample 3, with $\alpha = 5°$ yielding started at a load of 11 kN. After yielding, the alloy showed about 0.2 mm displacement and finally fractured at a load of 12.6 kN. It was also observed that load–displacement curve of conical samples exhibited serrations soon after yielding. The inset of Fig. 3 shows the magnified view of flow serrations. This serrated characteristic is an indication of simultaneous operation of multiple shear bands rather than a discrete shear band nucleation [20, 21].

Figure 4a shows SEM image of top view of fractured surface of cylindrical specimen (sample 1) after compression test, which indicates a typical vein-like morphology oriented in the same direction [22]. Formation of few non-intersecting shear bands (marked by arrows) was observed on the flat side of fractured surface as shown in Fig. 4b. Due to the formation of few non-interacting shear bands

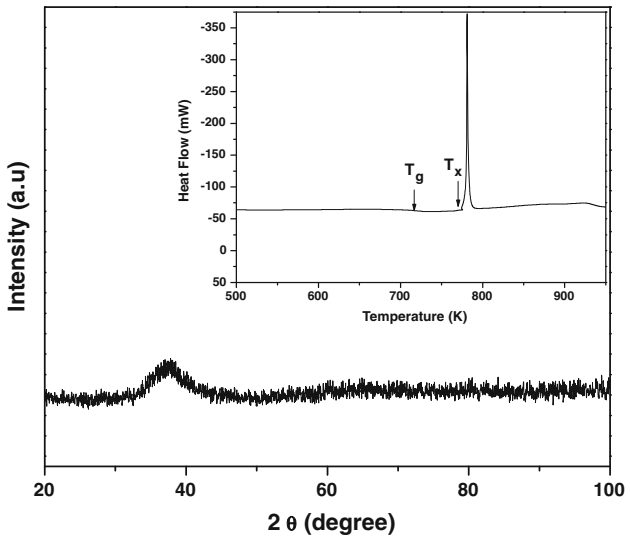

Fig. 2 XRD pattern of as-cast bulk amorphous alloy; *inset* shows DSC curve at a heating rate of 20 K/min

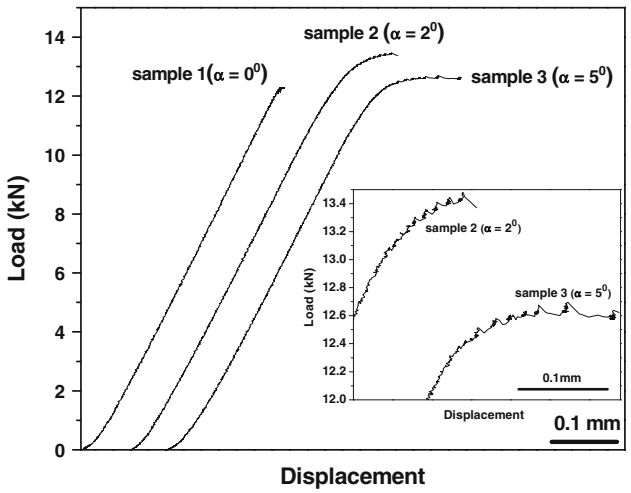

Fig. 3 Room temperature load–displacement curves for the alloy of different dimensions

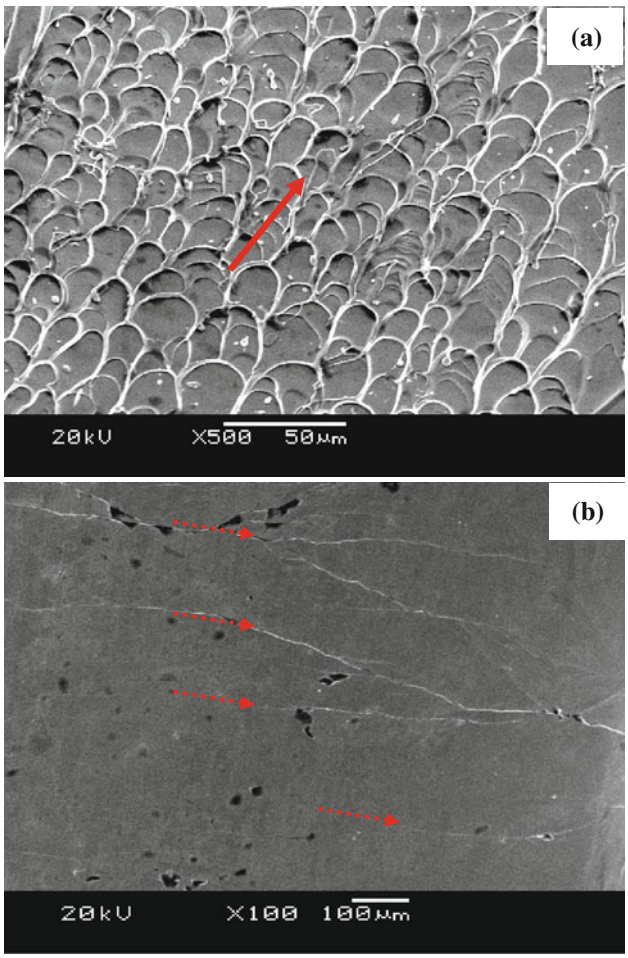

Fig. 4 SEM image of fractured surface of sample 1, showing typical vein-like pattern elongated in the same direction (**a**), SEM micrographs of flat side of fractured surface showing few parallel shear bands (**b**)

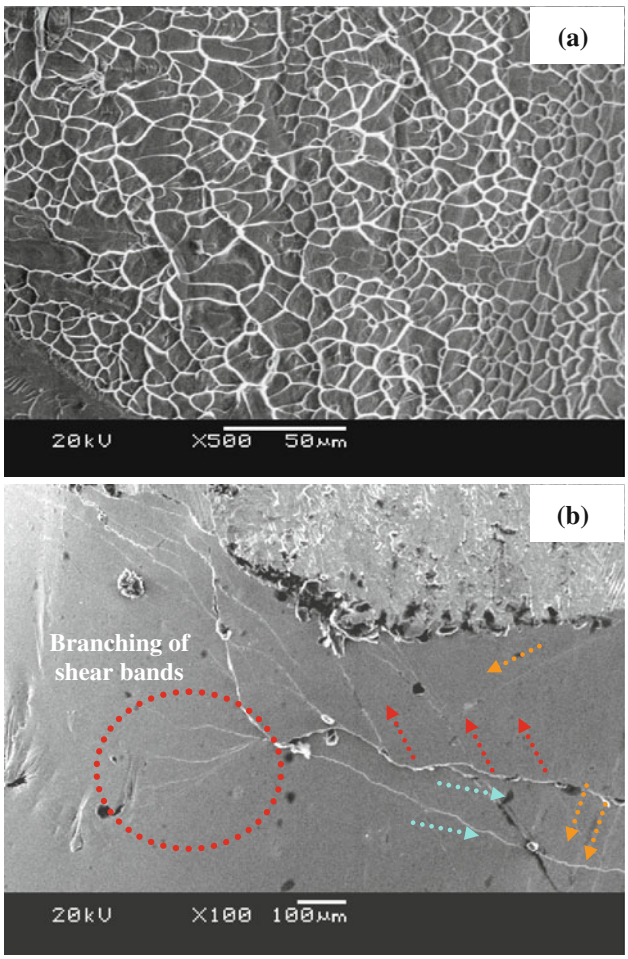

Fig. 5 SEM image of fractured surface of sample 2, showing distortion of veins (**a**), SEM micrographs of flat side of fractured surface showing intersection and branching of shear bands (**b**)

sample showed a brittle behavior and fractured catastrophically by one dominant shear band [23]. SEM image of fractured surface of geometrically constrained conical specimen (sample 2) is shown in Fig. 5a that indicates distortion of the vein-like morphology. Figure 5b shows multiple and branched shear bands on the flat side of the fractured surface of sample 2. This is also evident from the flow serrations of load–displacement curve. Geometrical constraints produce stress gradients in conical samples and prevent the excessive propagation of individual shear bands by promoting the multiplication and crosslinking of the shear bands. This results in substantial development of the plastic deformation [13, 18–20]. Figure 6a shows SEM image of fractured surface of sample 3 which indicates extreme distortion and branching of veins. It is quite interesting that with increasing semi-vertex angle (α) of conical sample from 2° to 5° more effective geometrical confinements took place in the sample. As a result, a complex multi-axial stress condition is induced in the sample that leads to the extensive generation of multiple shear bands intersecting in complex manner as shown in Fig. 6b [20]. This is also evident from the presence of few loops [5], secondary and tertiary branching of distorted veins (as circled in Fig. 6a) as well as complex serrated pattern in the load–displacement curve of sample 2 (Fig. 4b). This shows that with a slight change in the geometry of the sample, i.e., from cylindrical shape (for which $\alpha = 0$) to conical shape (for which $\alpha > 0$), a fully brittle BMG sample tends to deform in a ductile fashion. This change in deformation mode is attributed to the geometrical constraint (conical shape) induced complex triaxial stress distribution in the sample, which further leads to the extreme distortion and branching of shear veins as well as evolution of complex intersecting multiple shear bands that avoids the undesired catastrophic failure. The correlation of SEM observations with the load–displacement results clarifies very well the change in deformation behavior resulting from the geometrical constraints. The present findings are important from an application point of

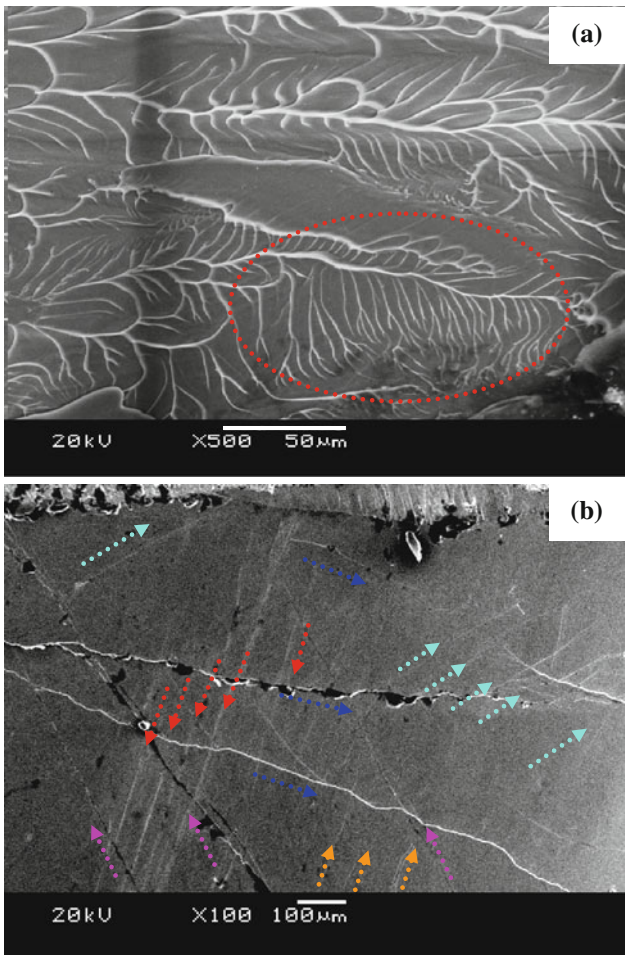

Fig. 6 SEM micrographs of fractured surface of sample 3, showing extreme distortion and branching of veins network (**a**), SEM micrographs of flat side of fractured surface showing complex intersection of multiple shear bands (**b**)

view as geometrical change of sample has shown very useful effect on the fracture behavior of the brittle BMG.

Conclusions

It is shown that the specimen geometry strongly influences the deformation behavior of $Zr_{57.5}Cu_{11.2}Ni_{13.8}Al_{17.5}$ BMG. As the geometry of the sample was changed from cylindrical shape (for which $\alpha = 0$) to conical shape (for which $\alpha > 0$) gradually, almost brittle BMG sample deformed in a ductile manner due to the geometrical constraint-induced complex stress distribution in the sample. The change in geometry led to the evolution of complex intersecting multiple shear bands useful for avoiding the catastrophic failure.

References

1. Greer AL (1995) Science 267:1947
2. Inoue A (2000) Acta Mater 48:279
3. Tariq NH, Iqbal M, Shaikh MA, Akhter JI, Ahmad M, Ali G, Hu ZQ (2008) J Alloys Compd 460:258
4. Johnson WL (1999) Mater Res Bull 24:42
5. Tariq NH, Hasan BA, Akhter JI, Shaikh MA (2009) J Alloys Compd 477:L8
6. Shamimi Nouri A, Gu XJ, Poon SJ, Shiflet GJ, Lewandowski JJ (2008) Philos Mag Lett 88:853
7. Sunny G, Lewandowski JJ, Prakash V (2007) J Mater Res 22:389
8. Lewandowski JJ, Shazly M, Nouri AS (2006) Scr Metall 54:337
9. Lewandowski JJ, Wang WH, Greer AL (2005) Philos Mag Lett 85:77
10. Gu XJ, Poon SJ, Shiflet GJ, Lewandowski JJ (2010) Acta Metall 58:1708
11. Sunny G, Yuan F, Prakash V, Lewandowski JJ (2009) Exp Mech 49:479
12. He L, Zhong MB, Han ZH, Zhao Q, Jiang F, Sun J (2008) Mater Sci Eng A 496:285
13. Lewandowski JJ, Lowhaphandu P (2002) Philos Mag A 82:3427
14. Bruck HA, Christman T, Rosakis AJ, Johnson WL (1994) Scr Metall Mater 30:429
15. Bei H, Xie S, George EP (2006) Phys Rev Lett 96:105503
16. Lu J, Ravichandran G (2003) J Mater Res 18:2039
17. Zhang ZF, Zhang H, Pan XF, Das J, Eckert J (2005) Philos Mag Lett 85:513
18. Jiang WH, Fan GJ, Choo H, Liaw PK (2006) Mater Lett 60:3537
19. Xie S, George EP (2008) Intermetallics 16:485
20. Wu WF, Zhang CY, Zhang YW, Zeng KY, Li Y (2008) Intermetallics 16:1190
21. Yao KF, Zhang CQ (2007) Appl Phys Lett 90:061901
22. Tariq NH, Hasan BA, Akhter JI, Ali F (2009) J Alloys Compd 469:179
23. Spaepen F (1977) Acta Metall 25:407